2404–2415 *Nucleic Acids Research, 2011, Vol. 39, No. 6* *Published online 13 November 2010*
doi:10.1093/nar/gkq979

Importance of the proline-rich multimerization domain on the oligomerization and nucleic acid binding properties of HIV-1 Vif

Serena Bernacchi*, Gaëlle Mercenne, Clémence Tournaire, Roland Marquet and Jean-Christophe Paillart*

Architecture et Réactivité de l'ARN, Université de Strasbourg, CNRS, Institut de Biologie Moléculaire et Cellulaire, 15 rue René Descartes, 67084 Strasbourg, France

Received July 13, 2010; Revised and Accepted October 4, 2010

ABSTRACT

The HIV-1 viral infectivity factor (Vif) is required for productive infection of non-permissive cells, including most natural HIV-1 targets, where it counteracts the antiviral activities of the cellular cytosine deaminases APOBEC-3G (A3G) and A3F. Vif is a multimeric protein and the conserved proline-rich domain ^{161}PPLP^{164} regulating Vif oligomerization is crucial for its function and viral infectivity. Here, we expressed and purified wild-type Vif and a mutant protein in which alanines were substituted for the proline residues of the ^{161}PPLP^{164} domain. Using dynamic light scattering, circular dichroism and fluorescence spectroscopy, we established the impact of these mutations on Vif oligomerization, secondary structure content and nucleic acids binding properties. *In vitro,* wild-type Vif formed oligomers of five to nine proteins, while Vif AALA formed dimers and/or trimers. Up to 40% of the unbound wild-type Vif protein appeared to be unfolded, but binding to the HIV-1 TAR apical loop promoted formation of β-sheets. Interestingly, alanine substitutions did not significantly affect the secondary structure of Vif, but they diminished its binding affinity and specificity for nucleic acids. Dynamic light scattering showed that Vif oligomerization, and interaction with folding-promoting nucleic acids, favor formation of high molecular mass complexes. These properties could be important for Vif functions involving RNAs.

INTRODUCTION

In addition to the three conserved retroviral protein precursors Gag, Pol and Env, the human immunodeficiency virus type 1 (HIV-1) encodes several regulatory (Tat, Rev and Nef) and auxiliary proteins (Vif, Vpr and Vpu), which are known to modulate the host environment and regulate the efficiency of viral replication and transmission (1). The HIV-1 virion infectivity factor (Vif), is a 23 kDa basic protein of 192 amino acids (2) that is absolutely required for productive infection of some cell types, named 'non-permissive', such as primary T-cells, monocytes and macrophages, (3–5). In those cells, Vif has been shown to efficiently counteract the antiviral activity of several APOBEC3 (APOlipoprotein B mRNA-editing enzyme catalytic polypeptide-like) cytidine deaminases by various mechanisms (6,7). Among the members of this enzyme family, APOBEC3G (A3G) and A3F display the highest antiviral activity (8–13). In the absence of Vif, these antiviral factors are incorporated into budding virions and promote cytosine deamination during (−) strand DNA synthesis. Besides, HIV-1 DNA synthesis and integration can also be impaired by A3G/3F irrespective of their catalytic activity, suggesting that deamination is not the only determinant for antiviral activity (6,12,14–16). In non-permissive cells, Vif targets A3G/3F for degradation by the proteasome by recruiting an E3 ubiquitin ligase cellular complex composed of Elongin B (EloB), Elongin C (EloC), Cullin 5 (Cul5) and RING-box protein 2 (Rbx2) (11,17–21). This is probably not the only mechanism used by Vif to neutralize A3G/3F antiviral effects. Indeed, it was observed that Vif can also (i) inhibit, directly or indirectly, packaging and antiviral activity of a degradation resistant A3G mutant (22); (ii)

*To whom correspondence should be addressed. Tel: + 33 3 88 41 70 40; Fax: + 33 3 88 60 22 18; Email: s.bernacchi@ibmc-cnrs.unistra.fr
Correspondence may also be addressed to Jean-Christophe Paillart. Tel: + 33 3 88 41 70 35; Fax: + 33 3 88 60 22 18; Email: jc.paillart@ibmc-cnrs.unistra.fr

The authors wish it to be known that, in their opinion, the first two authors should be regarded as joint First Authors.

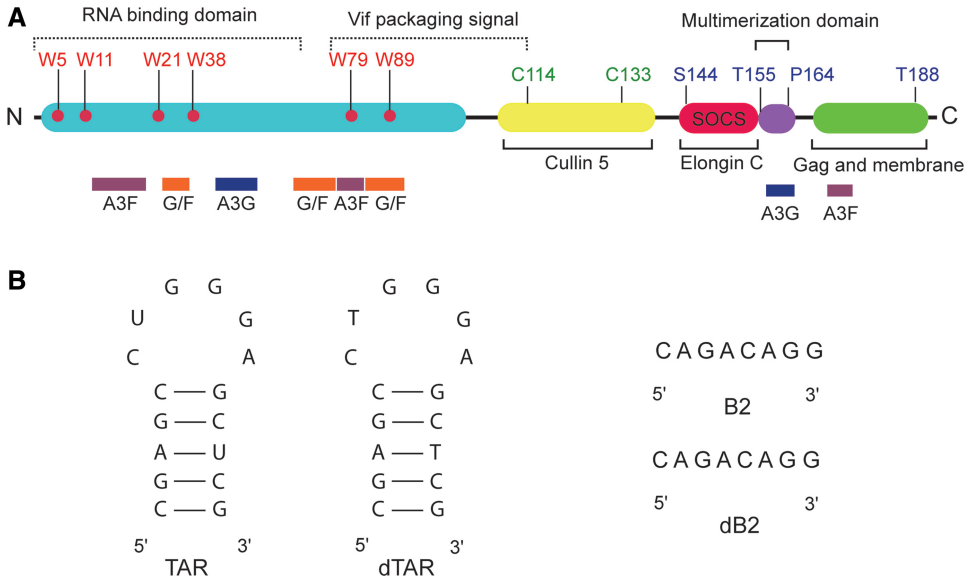

Figure 1. (**A**) Schematic representation of HIV-1 Vif domains required for interactions with viral and cellular partners. (**B**) Secondary structure of RNA sequences TAR, and its DNA analog, dTAR. Primary structure of fragment B2 encompassing genomic nucleotides 539–547, and its DNA analog dB2.

promote the incorporation of A3G into high molecular mass (HMM) complexes (23) and (iii) reduce intracellular expression of A3G (24,25). In this context, we recently showed that Vif down regulates A3G translation by binding to the 5′-UTR region of its mRNA (26).

Vif protein consists in several functional domains (Figure 1A). The N-terminal region corresponds to an RNA-binding domain, and contains discontinuous binding sites for A3G and A3F (17,27–31). Interestingly, this domain is rich in highly conserved tryptophan residues (32) that confer an intrinsic fluorescence signal to Vif. It has been shown that Vif possesses an RNA chaperone activity (33) and binds specifically and cooperatively the 5′-end region of HIV-1 genomic RNA *in vitro* (34,35) and in infected cells (36,37). Next to these RNA and A3G/3F binding domains, the HCCH motif (residues 108–139) coordinates a Zn^{2+} ion (Figure 1A). This motif, together with the following highly conserved ^{144}SLQYLA^{149} domain (38) plays a crucial role in A3G/F protein inactivation (39,40). Indeed, these regions bind directly to Cul5 and EloBC factors (20,41,42) (Figure 1A), leading to A3G/F degradation by the proteasome (43). Next, region 151–164 encompasses the conserved proline-rich region ^{161}PPLP^{164} that governs Vif multimerization (Figure 1A) (44,45). Indeed, Vif has been shown to self-associate and to form dimers, trimers and tetramers *in vitro* (44,46), as well as in cells (44). This short domain was found to be crucial for Vif function and viral infectivity (44,45,47). Moreover, it can interact with A3G (48,49), Cul5 (39) and HIV-1 reverse transcriptase (50). Recently, it was also observed that an intact PPLP motif is required for interaction with EloB (51,52). In this context, it is conceivable that these functions are linked to the multimerization state of Vif. Finally, it was observed that Vif exists in both membrane-associated and cytoplasmic forms (53), and mutagenesis studies demonstrate that these functions could be attributed to the C-terminal basic domain of Vif, which also interacts with the Pr55^{Gag} precursor (Figure 1A) (47,53,54).

In the cytoplasm, Vif was also found to be a component of an RNP complex containing cellular and viral factors like genomic RNA and Pr55^{Gag} (36,37,55). Interestingly, these interactions with viral RNA and Pr55^{Gag} are responsible for Vif incorporation into viral particles (55,56). Moreover, Vif(−) virions are affected in their morphology and reverse transcription (57,58). The deficiency in proviral DNA synthesis could result from the destabilization of the viral core, suggesting that Vif association to RNA might mediate genome engagement with Pr55^{Gag} precursor in the assembly complex (6,59).

While numerous studies contributed to investigate the multiple functions of Vif, there is still a lack of information concerning its tridimensional structure (43). To date, the only available 3D structure corresponds to peptide 139–179 in association with an EloB/C complex (60). Theoretical predictions provided structural information on Vif domains, and homology models and disorder prediction studies contributed to predict the overall tertiary structure of N- and C-terminal domains (43,46,61,62). Recently, other studies combining circular dichroism (CD) and dynamic light scattering (DLS) provided conformational analysis of a peptide approximating the HCCH motif (63,64) and the C-terminal domain of Vif (65). Nevertheless, there still remains a lack of structural information of Vif protein in its unbound state and in interaction with nucleic acids, as well. One of the major limitations resides in difficulties in expressing and purifying full-length HIV-1 Vif proteins. Here, we described the expression and purification of wild-type HIV-1 Vif protein and a mutant form in which the proline-rich domain leading to Vif multimerization was replaced by alanines (Vif AALA). Conformational investigations, secondary

structure content and analysis of binding parameters to high-affinity RNA and DNA sites were characterized by biophysical techniques including DLS, CD and fluorescence spectroscopy. We provide evidence of unstructured regions in unbound Vif, and show that upon binding to the HIV-1 TAR apical loop, the unfolded content of Vif decreases. This was not the case for other primary binding sites. Interestingly, the alanine substitutions in the Vif PPLP motif did not significantly affect the overall secondary structure of the protein, but it decreased the binding affinity and specificity for nucleic acids. Finally, conformational analysis of ribonucleoprotein complexes showed that Vif oligomerization, as well as its binding to folding-promoting nucleic acids, are required to promote the formation of HMM complexes.

MATERIALS AND METHODS

Recombinant Vif proteins

Expression plasmids pD10WT-Vif or pD10AALA-Vif were used to transform *Escherichia coli* BL21 cells as described earlier (26). Briefly, production of Vif proteins was induced by addition of 0.5 mM IPTG to log phase bacterial cultures (OD_{600nm} = 0.4–0.6). After 6 h at 22°C for wild-type Vif or at 16°C in the case of Vif AALA, bacteria were harvested by centrifugation at 4000*g* during 15 min, lysed in the denaturating lysis buffer (6M guanidine hydrochloride, 100 mM sodium phosphate, 10 mM Tris, pH 8) at room temperature and stirred overnight. Cellular debris was separated by centrifugation at 27000*g* during 30 min at 4°C and the cleared lysate was loaded onto a Ni-NTA agarose column (Invitrogen). The column was washed with the lysis buffer and elution was performed by pH decreasing (from 6.5 to 4.5). Fractions containing Vif proteins were analyzed on 12% SDS–PAGE and pooled. Proteins were then renatured by slow dialysis against buffers with decreasing guadinium chloride concentration, and finally against a buffer containing 50 mM MOPS pH 6.5, 150 mM NaCl, 10% glycerol. This last buffer was supplemented with 550 mM arginine during the dialysis step to avoid the precipitation of Vif AALA protein. As both wild-type Vif and Vif AALA tend to aggregate, protein stock solutions were centrifuged at 100 000*g* for 30 min at 4°C immediately prior to use. The protein concentration in the supernatant was determined spectrophotometrically and UV spectroscopy revealed that purified Vif proteins were not contaminated by nucleic acids.

Size exclusion chromatography

Gel filtration chromatography was performed at 25°C on a Superdex 75 (Pharmacia) in an AKTA purifier FPLC (GE Healthcare Biosciences, UK). The running buffer was 50 mM NaCl, 50 mM MOPS, 10% glycerol, 0,5 mM Tween-80, 2 mM DTT for wild-type Vif protein and 150 mM NaCl, 50 mM MOPS, 10% glycerol, 2 mM DTT for Vif AALA protein. The gel filtration column was calibrated in the different buffers used for analysis with molecular mass markers (thyroglobulin 670 kDa, bovine γ-globulin 158 kDa, chicken ovalbumin 44 kDa, equine myoglobin 17 kDa and vitamine B12 1350 Da). Protein elution was monitored at 280 nm and results were analyzed using Unicorn software (version 4.11).

RNA and DNA oligonucleotides

Plasmid pHXB2 was used as a template to amplify 500 bp DNA fragments corresponding to the 5′-UTR (RNA A), a part of *gag* gene (RNA B), and 3′-UTR (RNA H) regions of the HIV-1 genome. Pairs of sense and antisense primers were used in PCR reactions and products were digested and inserted into pUC18 as described in ref. (34). Plasmids were linearized and used as template for *in vitro* transcription with bacteriophage T7 RNA polymerase. Reaction mixture was incubated with RNase-free DNase I (Qbiogen), extracted with phenol, and precipitated in ethanol. RNAs were then purified by FPLC (Amersham Biosciences Inc.) and dissolved in water.

Three RNA oligonucleotides corresponding to a C_{10} sequence, the TAR apical loop and RNA B2 (a single-stranded sequence located between nucleotides 539 and 546 of the HIV-1 genomic RNA) (35) (Figure 1B) were synthesized by Microsynth (Balgach, Switzerland) and purified by anion exchange HPLC on a nucleo-PAC PA-100 column (Dionex Co). Their DNA counterparts were synthesized and purified by reverse-phase HPLC (ThermoFisher Scientific, Ulm-Germany).

Diffusion light scattering

Wild-type Vif and Vif AALA samples were prepared in 50 mM MOPS, 150 mM NaCl, pH 6.5 at a final concentration of 15 μM. Intensities of scattered light and correlation times were measured with a Zetasizer Nano S (Malvern, UK). Measurements were performed in a single 50 μl trUView cuvette (Biorad Laboratories, CA, USA), maintained at 25°C. Diffusion light scattering (DLS) fluctuations of the scattering intensity due to Brownian motion were recorded at microsecond time intervals. An autocorrelation function was derived, thus leading to the determination of diffusion coefficients. Assimilating proteins in solution to spheres, diffusion coefficients were related to the hydrodynamic radius of the particles, R_h via the Stokes–Einstein equation:

$$D = \frac{kT}{R_h 6\pi\mu} \quad (1)$$

in which k is the Boltzmann constant, T the temperature (K), μ the solvent viscosity and D the translational diffusion coefficient. All experimental data were corrected for solvent viscosity (measured with a 3.5 ml micro-Ubbelohde capillary viscosimeter tube from Schott, Germany), and refractive index (measured with an Abbé refractometer). Size measurements by DLS have been used to monitor the assembly of Vif proteins and oligonucleotides. Increasing amounts of nucleic acids (protein/nucleic acid ratio, R varying from 0 to 2) were added to a fixed amount of wild-type Vif protein (between 10 and 15 μM). Scattering data of Vif proteins and protein/oligonucleotide complexes were then analyzed using DLS analysis software (Malvern, UK).

Circular dichroism

Wild-type Vif and Vif AALA (10 μM) protein samples were prepared anaerobically in 50 mM MOPS, 150 mM NaCl, pH 6.5 at a final concentration of 15 μM. Far-UV CD spectra (190–250 nm) were measured in a Jasco J-810 spectropolarimeter (Jasco Inc., Easton, MD, USA). Samples were placed in rectangular quartz cuvettes of 2-mm path length maintained at 20°C. Spectra were acquired at 50 nm/min with a time constant of 1s and band-width equal to 1. Each spectrum represents the average of 15 successive baseline-corrected scans. The mean residue molar ellipticity [Θ] was determined according to:

$$[\Theta] = (\Theta \cdot M_R)/(10 \cdot \lambda \cdot c) \quad (2)$$

where Θ is the measured ellipticity in millidegrees, M_R is the mean residue mass, λ the optical path length and c, the protein concentration. For wild-type Vif, equimolecular amounts of nucleic acid were added directly in the cell measure. Corresponding spectra were corrected for nucleic acids absorbance and ellipticity. Deconvolution of far-UV CD spectra and consequent secondary structure of proteins content was estimated by Dichroweb (http://dichroweb.cryst.bbk.ac.uk/html/home.shtml).

Steady state fluorescence measurements

Fluorescence measurements were recorded in quartz cells at 20 ± 0.2°C on a Fluoromax-4 fluorometer (HORIBA Jobin-Yvon Inc., NJ, USA). The excitation wavelength was set at 295 nm for selective excitation of Trp residues. The emission wavelength was scanned from 310 to 450 nm; the integration time was 0.1s, and the excitation and emission bandwidths were 5 nm. Fluorescence titrations were performed by adding increasing amounts of nucleic acid to 100 nM Vif in 30 mM Tris–HCl (pH 7.5), 200 mM NaCl and 10 mM $MgCl_2$. Fluorescence intensities were corrected for buffer fluorescence and dilution effect.

To determine the binding parameters of Vif proteins to genomic RNA fragments, we measured the decrease of the fluorescence intensity, I, at a fixed concentration of protein in presence of increasing RNA concentrations. The fluorescence intensity was then converted into the intrinsic fluorescence quenching Q_{obs}:

$$Q_{obs} = \frac{I_0 - I}{I_0} \quad (3)$$

with I_0 corresponding to the protein fluorescence intensity in absence of nucleic acid.

Scatchard equation was used to fit the protein/nucleic acid titration data (66):

$$v = \frac{n K_{obs} L}{1 + K_{obs} L} \quad (4)$$

where L corresponds to the free protein concentration which is obtained by:

$$L = L_t - vN_t \quad (5)$$

Finally, the average number v of protein bound per oligonucleotides was determined using:

$$v = \frac{(I_0 - I)}{(I_0 - I_f)} \frac{L_t}{N_t} \quad (6)$$

where L_t and N_t correspond to the total concentration of protein and oligonucleotide, respectively, and I_f is the fluorescence intensity at the *plateau* when all the proteins are bound to the nucleic acid.

The model of McGhee and von Hippel for cooperative binding (67), was used to fit protein/genomic RNA fragment titration data:

$$\frac{v}{L} = K_{obs} \cdot (1 - nv) \times \cdot \frac{[(2\omega - 1)(1 - nv) + v - R]^{n-1}}{[2(\omega - 1)(1 - nv)]^{n-1}} \cdot \frac{[1 - (n+1)v + R]^2}{[2(1 - nv)]^2} \quad (7)$$

with $R = \left\{[1 - (n+1)v]^2 + 4\omega v(1 - nv)\right\}^{1/2}$

Where n corresponds to the number of consecutive nucleotides occluded upon binding of one ligand, and ω, to the cooperativity parameter. Because the McGhee and von Hippel (67) model was derived with the simplifying assumption of an infinite lattice of binding sites, we introduced a correction factor taking into account the finite lattice size, N. The correction merely amounts to multiplying Equation 7 by the factor $(N-n+1)/(N)$ (68). Curve fitting was performed using Mathematica software (Wolfram Research Inc, Champaign, IL, USA).

RESULTS

The PPLP motif contributes to Vif oligomerization

We first focused on Vif protein characterization, and in particular, we wished to establish the impact of the PPLP motif on Vif self-association. Prior to each analysis, proteins were centrifuged as described (26) and soluble fractions were used to determine the oligomerization state of the proteins by size exclusion chromatography and DLS. Wild-type Vif protein had an apparent molecular weight of 209 kDa (Figure 2A), as judged by its elution volume from the size exclusion chromatography column (11.25 ml), suggesting that Vif is organized as a complex of about nine proteins (Figure 2C). On the contrary, Vif AALA assembles as a complex of 76 kDa (Figure 2B), thus containing about three proteins (Figure 2C). Next, we characterized Vif proteins by DLS. Assuming that Vif proteins in solution can be considered as spherical particles, the diffusion coefficient could be related to their hydrodynamic radius *via* the Stokes–Einstein equation (Equation1). For wild-type Vif, we observed a mean radius of 5.3 ± 0.6 nm (Figure 3A), which corresponds to about 5–8 Vif proteins. Differently, Vif AALA mutant protein showed a mean radius of 3.2 ± 0.3 nm, which can most likely be assigned to protein dimers (Figure 3B). Altogether, both techniques gave similar results and showed that proline to alanine substitutions strongly reduce the capacity of Vif to multimerize, and

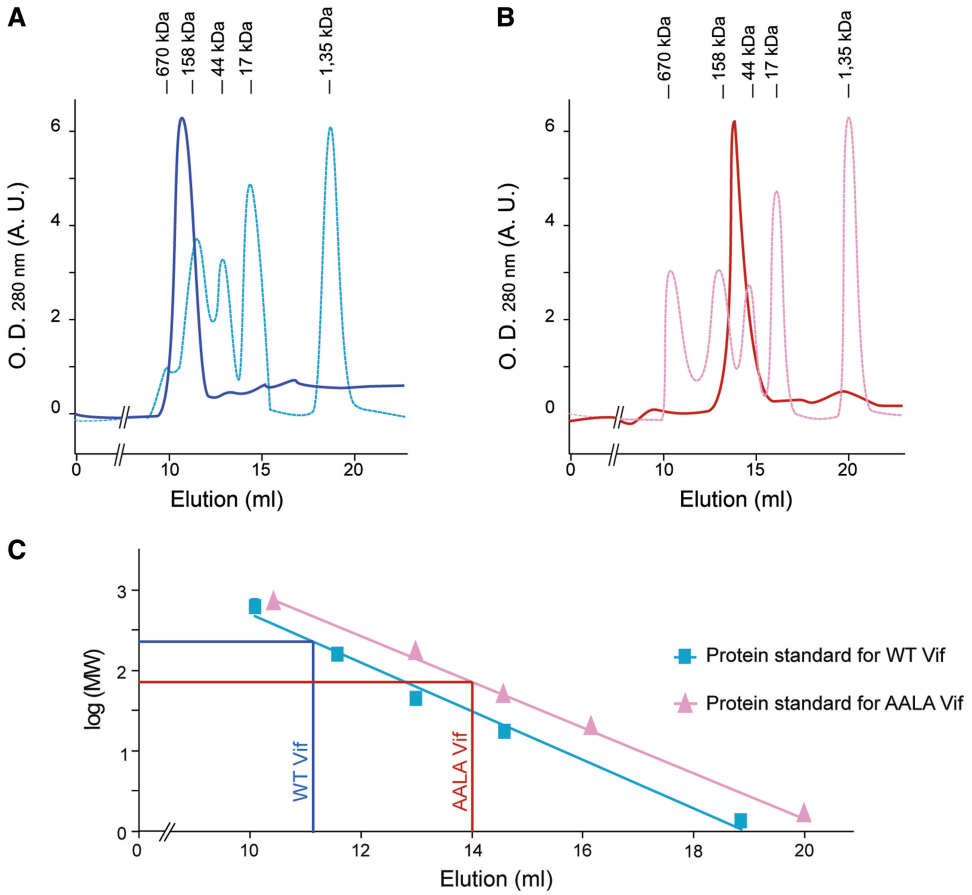

Figure 2. Size exclusion chromatography on wild-type and mutant Vif proteins. Elution profiles of Vif wild-type (**A**) and Vif AALA (**B**) are represented together with protein standards. (**C**) The molecular weights (log) are plotted against elution volumes calibrated using molecular weight standards. Measured molecular weights of Vif wild-type and Vif AALA give 209 kDa and 76 kDa, respectively, corresponding to about 9 and 3 Vif proteins in each complex.

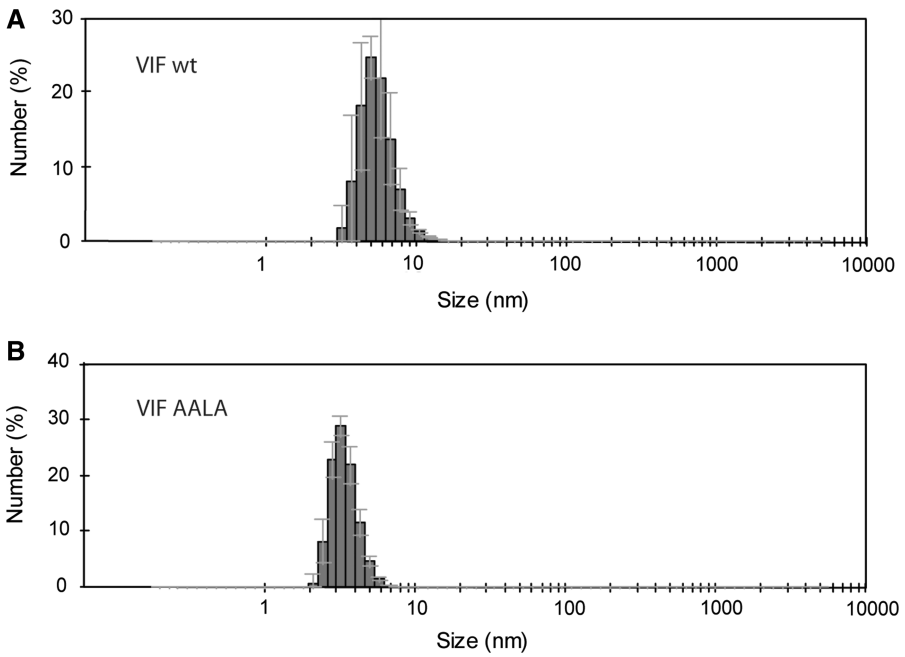

Figure 3. Diffusion light scattering profiles of wild-type Vif (**A**) and Vif AALA (**B**) proteins. (**A**) Mean radius for wild-type protein was 5.3 ± 0.6 nm, which corresponds to polymers containing 5 to 8 Vif proteins. (**B**) Vif AALA proteins showed a mean radius of 3.2 ± 0.3 nm, mainly corresponding to dimers of Vif.

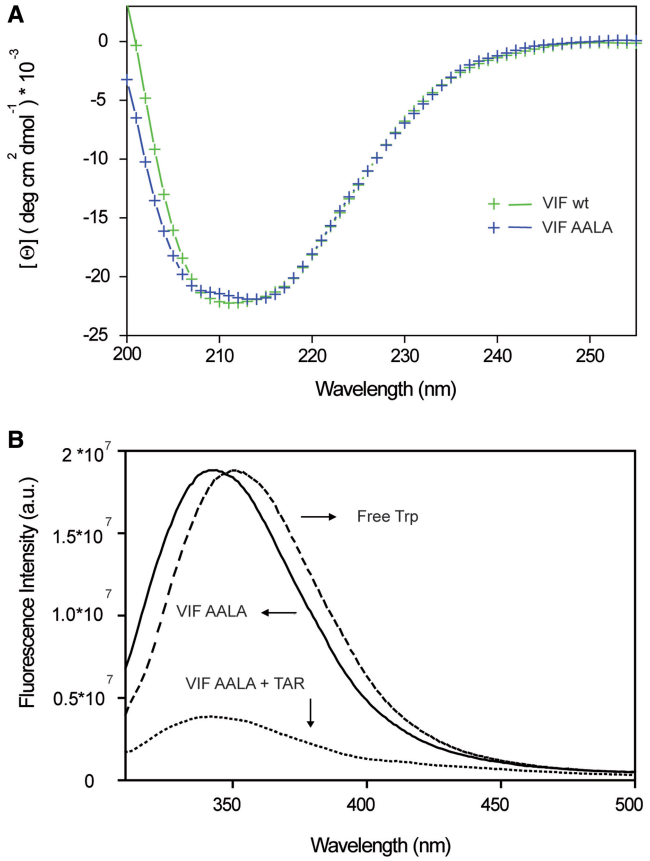

Figure 4. Influence of Vif oligomerization on its secondary structure content and fluorescence properties. (**A**) Far-UV-CD spectra of wild-type (green) and AALA mutant (blue) Vif proteins. Proteins were prepared at a final concentration of 10 μM. (**B**) Emission fluorescence spectra of free Trp amino acid (dashed line), free Vif AALA protein in solution (solid line) and in complex with TAR fragment (dotted line). Excitation wavelength was set at 295 nm.

demonstrate that the PPLP motif contributes to the oligomerization of the Vif protein. However, the mutant protein was still able to dimerize, indicating that other regions of Vif also contribute to multimerization.

The oligomerization state of Vif influences neither its secondary structure nor its fluorescence properties

Because amino acid changes can often affect secondary structure of proteins, we next analyzed wild-type and Vif AALA proteins by UV-CD spectroscopy to determine their secondary structural content. Analysis of the UV-CD spectrum for wild-type protein revealed that the HIV-1 Vif contains 41.5% β-sheet, 6.5% α-helix, 40% random coil, and the remaining 12% are turns (Figure 4A). The secondary structure content of Vif AALA protein was rather similar: we observed nearly identical fractions of β-sheet (42%) and random coil (46%), and a slight decrease in α-helical content (5%), and turns (7%). Taken together these data suggest that mutation of the proline-rich domain in Vif does not significantly affect the overall secondary structure of the protein (Figure 4A).

Trp residues constitute very sensitive probes for investigating protein/nucleic acid interactions because of their high quantum yield and sensitivity to the physicochemical environment (69). Vif contains six Trp residues in its N-terminal domain, which corresponds to the RNA binding region (37) (Figure 1A). We have observed earlier that after selective excitation of Trp residues at 295 nm, the emission spectrum revealed a maximum at 338 nm (35). Vif AALA presented its maximal emission at 340 nm (Figure 4B). Free Trp amino acid in solution displayed a fluorescence emission maximum at 350 nm, and the blue shifts of the emission maximum of wild-type and Vif AALA revealed that Trp residues in both proteins are mainly located in a non-polar environment (70). This shows that mutation of the Vif PPLP motif does not significantly interfere with the local environment of Trp residues. Moreover, upon nucleic acid binding, the wavelength of maximal fluorescence emission of Vif AALA was unchanged, whereas the fluorescence intensity decreased depending on the nucleic acid sequences and concentration (Figure 4B).

Mutation of the PPLP motif of Vif decreases its affinity and specificity toward HIV-1 RNA

We showed earlier that Vif is an RNA binding protein that binds specifically the 5′-terminal region of HIV-1 genomic RNA (34,35). Here, we asked whether Vif multimerization is involved in this process. To this aim, we synthesized *in vitro* a set of genomic RNA fragments of ~500 nt in length corresponding to parts of the *gag* coding regions (RNA A and RNA B) or containing the polypurine tract (PPT), which constitutes the primer for (+) strand DNA synthesis during reverse transcription (RNA H) (Table 1) (34). Reverse titrations were performed by adding small volumes of concentrated RNA solutions to a fixed amount of protein, and protein binding was monitored through the decrease of Vif AALA intrinsic fluorescence resulting from protein/nucleic acid complex formation. According to our earlier results (35), best fit of our experimental data was obtained with a cooperative model (Equation 7) (67). Fluorescence titrations revealed a decrease of Vif AALA fluorescence of ~70–75% (Table 1). Analysis of the equilibrium dissociation constants, K_d, showed that Vif AALA had a similar affinity for RNA fragments A, B and H (Table 1). In addition, protein binding to RNAs A and B was moderately more cooperative (ω ~85–110) compared with binding to RNA H (ω ~65). Finally, the binding stoichiometry of Vif AALA, given by the intersection of the initial slope of the titration curves with the fluorescence plateau (data not shown), was about 10 Vif proteins for all RNAs. On the opposite, wild-type Vif protein displayed higher fluorescence quenching, affinity and binding cooperativity values for RNAs A and B (Qmax ~77%, K_d ~45–55 nM, and ω ~65–80) compared with RNA H (Qmax ~ 47%, K_d ~165 nM, ω ~17) (35). Moreover, ~45 wild-type Vif proteins bound to RNAs A and B, and about 20 bound to RNA H (35). Taken together these results suggest that mutation of the PPLP motif

Table 1. Vif AALA and wild-type VIF binding parameters RNA genomic fragments

RNA	Genomic region	VIF AALA			HIV-1 VIF		
		K_d (nM)[a]	ω[a]	Q%	K_d [b]	ω[b]	Q%[b]
A	1–497	40 ± 7	107 ± 28	71	57 ± 7	68 ± 4	76
B	499–996	37 ± 4	85 ± 15	75	45 ± 4	80 ± 3	77
H	8625–9181	56 ± 9	60 ± 11	71	167 ± 6	17 ± 3	47

The maximum fluorescence quenching, Qmax, the cooperativity parameter, ω, and the equilibrium dissociation constants, K_d were obtained as described under 'Materials and Methods' section.
[a]Mean ± SD of at least three experiments.
[b]Binding parameters relative to wild-type Vif protein and genomic RNA fragments were published earlier in reference (35).

Table 2. Characterization of Vif AALA and wild–type VIF binding to RNA and DNA oligonucleotides

	VIF AALA		HIV-1 VIF	
	K_{sca} (nM)[a] RNA	DNA	K_{sca} (nM)[a] RNA	DNA
TAR/dTAR	37 ± 1	36 ± 1	9.5 ± 2.2[b]	9.5 ± 2.3[b]
B2/dB2	32 ± 2	39 ± 2	13 ± 2[b]	11 ± 2[b]
C10/dC10	61 ± 2	69 ± 2	59 ± 3	48 ± 2[b]

Determination of the apparent dissociation constants (K_{sca}) of Vif proteins was realized using the Scatchard model (66)
[a]Mean ± SD of at least three experiments.
[b]Binding parameters relative to wild-type Vif protein and RNA/DNA oligonucleotides were previously published in reference (35).

significantly decreases the overall affinity and specificity of Vif for viral RNA.

Vif AALA has lower affinity than wild-type Vif for minimal nucleic acids

We previously identified and characterized several minimal high affinity binding sites of wild-type Vif to HIV-1 RNA fragments (35). Here, we analyzed the binding of Vif AALA to two of them: the apical region of the trans-activation responsive element (TAR), a stable stem-loop structure located at the 5′-end of the viral genome (71), and a single-stranded segment (B2) encompassing nucleotides 539–547 of HIV-1 *gag* gene (Figure 1B). As a negative control, we analyzed Vif AALA binding to a C_{10} oligonucleotide, which was shown earlier to bind modestly wild-type Vif protein (35). According to our previous experiments (35), we expected that only one protein would bind to these oligonucleotides, and thus experimental data were fitted with a model for non-interacting ligands to a finite lattice (Equation 4) (66). Data analysis revealed very similar binding parameters for TAR and B2 oligoribonucleotides (K_d ~32–37 nM, Table 2). Compared with wild-type protein, Vif AALA presented 3 to 4-fold lower affinity for TAR and oligo B2 (K_d ~9.5–13 nM, Table 2) (35). However, both proteins showed very similar equilibrium dissociation constants for C_{10} (K_d ~60 nM, Table 2). We next extended our analysis to DNA counterparts of these RNA minimal binding sites (Figure 1B). Indeed Vif binding to DNA sequences might protect HIV-1 genome by neutralizing A3G/3F antiviral activity by competition mechanisms (34). Analysis of dissociation constants of Vif AALA for dTAR and dB2 showed similar K_d values (K_d ~36−39 nM, Table 2) compared with their RNA analogs, and 3- to 4-fold weaker affinities (K_d ~9.5–11 nM, Table 2) compared with the wild-type protein (35). Finally, the affinity of Vif AALA for dC_{10} was almost 2-fold lower than the ones observed for dTAR and dB2 oligonucleotides (Table 2). Compared with the wild-type protein, Vif AALA showed a weaker affinity for specific RNA and DNA binding sites, indicating that the PPLP motif plays a significant role in the specificity of interaction with nucleic acids.

Table 3. Determination of secondary structure contents of wild-type Vif protein bound to RNA and DNA oligonucleotides

	R	α-helical (%)	β-sheet (%)	Turns (%)	Random (%)
	0	6.5	41.5	12	40
TAR	1	4.5	69.5	7	19
B2	1	4	46	6	44
C10	1	5	41	11	43
dTAR	1	10	54	6	30
dB2	1	8	45	12	35
dC10	1	6	40	12	42

Equimolecular amounts of nucleic acids were added to wild-type Vif protein (R = 1). Spectra were corrected for nucleic acids ellipticity.

Interaction of wild-type Vif with RNAs promoting protein folding is a determinant of HMM complex formation

We next analyzed the secondary structure content of wild-type Vif protein in association with equimolecular amount of RNA and DNA oligonucleotides. Corresponding CD spectra were first corrected for nucleic acids absorbance and ellipticity before analysis. When TAR oligoribonucleotide was added to wild-type Vif, changes in CD spectra indicated a significant decrease in random coil content (from 40% to 19%) and turns (from 12% to 7%,), while β-sheets secondary structures increased from 41.5% to 69.5% (Table 3), and proportion of α-helical forms slightly decreased (from 6.5% to 4.5%). Vif binding to B2 oligoribonucleotide was characterized by a 2-fold decrease of turns (12–6%) and a slight decrease in α-heliticity (2.5%); however, this was offset by a moderate increase in β-sheet (41.5–46%) and random coil (40–44%) content. Binding to C_{10} RNA gave only very slight changes in protein secondary structure content (Table 3). On the contrary, when dTAR was added to Vif protein, the changes in CD spectra indicated an increase in structured content (α-heliticity from 6.5% to 10%, and β-sheet from 41.5% to 54%, Table 3), in parallel to a decrease of turns and random coils (12% to 6% and 40% to 30%, respectively). In agreement with results obtained with RNA oligonucleotides, Vif binding to dB2 led to a moderate increase in secondary structure content.

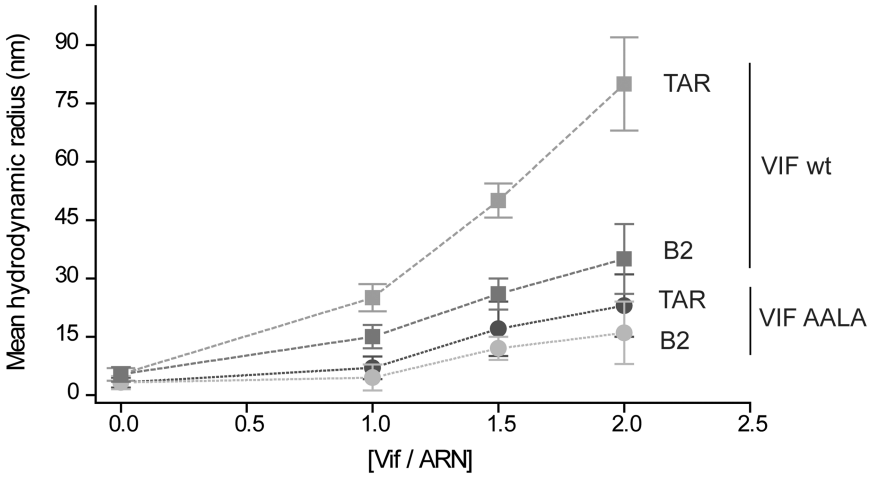

Figure 5. Ribonucleoprotein complexes were characterized by DLS. Increasing concentration of wild-type Vif were added to various amounts of oligoribonucleotides TAR and B2 (R RNA/protein ratio varying between 0 and 2). Similarly, TAR and B2 were added to Vif AALA. Protein/nucleic acid complex formation resulted in increasing complex radius.

Finally, binding to dC_{10} produced only minor structural changes (Table 3).

We further characterized ribonucleoprotein complexes by DLS. Vif proteins were mixed with increasing amount of TAR and B2 oligoribonucleotides (molar ratio *R* varied between 0 and 2) and we measured the hydrodynamic radius of the complex. In the case of wild-type Vif protein, at the highest *R*-value, Vif/TAR complexes were characterized by a mean radius almost 2-fold higher than the one measured for Vif/B2 complexes under the same conditions (Figure 5). On the contrary, in the case of Vif AALA, the radius of ribonucleoprotein complexes was similar for TAR and B2 sequences. Moreover, as expected from its oligomerization defect, the average size of Vif AALA/RNA complexes was lower than the one observed for wild-type Vif protein at equivalent molar ratio (Figure 5). Taken together, these results are consistent with a model where binding of Vif to specific RNA binding sites, such as the TAR element, may help the protein to adopt a more structured, and probably functional, conformation. Moreover oligomerization and interaction with nucleic acids that induce protein folding are important determinants for the formation of HMM ribonucleoprotein complexes.

DISCUSSION

HIV-1 Vif protein has been shown to form oligomers both *in vitro* and *in vivo* (44,46). The multimerization of Vif involves a sequence mapping between residues 151 to 164 in the C-terminal domain, and more precisely the ^{161}PPLP^{164} motif (44,45). Interestingly, disruption of this domain inhibited A3G degradation, and consequently increased its incorporation into viral particles, resulting in a loss of viral infectivity (44,48,49). Recently the PPLP motif was found to be required for the assembly of an active E3 ubiquitin ligase complex by interacting with the C-terminal domain of EloB (51,52). In this context, the oligomerization of Vif mediated by its proline-rich motif appears as an interesting target for developing therapeutic anti-HIV-1 drugs.

In this work, we expressed and purified wild-type HIV-1 Vif protein and a Vif mutant in which proline residues in the ^{161}PPLP^{164} domain were replaced by alanines. In order to precisely establish the impact of these mutations on Vif oligomerization, conformation and nucleic acids binding properties, we first characterized the oligomerization state of Vif proteins. Assuming that proteins in solution can be assimilated to spherical particles, we could determine their hydrodynamic radius by DLS. This analysis confirmed that *in vitro* wild-type Vif forms multimers containing 5–8 proteins (Figure 3A) (44,46). The same analysis applied to Vif AALA revealed that mutation of residues 161–164 mainly resulted in the formation of Vif dimers (Figure 3B). These results are in good agreement with the average molecular weight of wild-type Vif and Vif AALA determined by size exclusion chromatography (Figure 2), which showed that the two proteins could be organized as a complex of about 9 and 3 proteins, respectively (Figure 2C). Hence, even if oligomerization is considerably diminished in mutated proteins, it is not completely abolished, suggesting that regions outside the PPLP domain are also involved in protein–protein association. In this context, conformational analysis of a peptide corresponding to the HCCH motif of HIV-1 Vif showed that this Zn-binding domain could induce protein–protein interactions upon zinc binding. Indeed, metal binding increased formation of β-sheets, thus promoting protein self-association (63).

To gain insight into the secondary structure content of wild-type and mutant Vif proteins, we performed near-UV-CD spectroscopy. We observed that wild-type Vif contains nearly identical amounts of β-sheet (41.5%) and random coil (40%), only 6.5% α-helices and 12% of turns (Figure 4 and Table 3). The presence of large unfolded regions in Vif protein is consistent with previous studies, which provided evidence for the unstructured nature of its unbound C-terminal domain

(46,61,65,72). Natively unfolded regions confer high net charge and low overall hydrophobicity to proteins (73). Moreover, these unstructured domains are usually useful to mediate sequential/differential binding with multiple partners by inducing conformational changes for specific interaction (74,75). Indeed, it has recently been shown that intrinsic unstructured regions of Vif could be important for its interaction with an E3 ubiquitin ligase complex (64) and with EloC, resulting in this case in α-helix folding (51,60). Similar analysis on Vif AALA showed that both proteins have very similar secondary structure content, indicating that mutation of the proline-rich domain, which induces substantial changes of Vif quaternary structure, does not significantly affect its overall secondary organization (Figure 4).

Cross-linking experiments showed that contrary to the mainly unfolded C-terminal region, the N-terminal domain possesses a well-defined topology (46). This domain contains highly conserved tryptophan residues (32) that allowed us to compare fluorescence profiles of free Trp amino acids in solution (70), and Trp residues in Vif AALA (Figure 4B) and wild-type Vif proteins (35). Our results showed similar burial of those residues in wild-type and mutant proteins, suggesting that modification of the oligomerization state of Vif does not interfere with local environment of Trp residues, and consequently on the tertiary structure of Vif N-terminal domain. However, the replacement of prolines by alanines reduced the tendency of Vif to oligomerize in favor of protein dimers. Proline residues are known to form bends and kinks in proteins, and the PPLP motif could behave as a hinge between Vif domains leading to protein self-association. Our data support the idea that structural domains of Vif likely fold independently of each other, since alanine substitutions did not affect secondary and tertiary structure of the adjacent Vif domains. Moreover, the increased flexibility of the protein backbone due to alanine replacement would probably modify reciprocal spatial orientation of protein domains thus diminishing Vif tendency to oligomerization.

We previously showed that Vif specifically interacts with the 5′-region of HIV-1 genomic RNA (34,35) and with A3G mRNA (26). In particular, Vif binding to the 5′-UTR of A3G mRNA might be crucial for down-regulating A3G translation and may participate, together with the proteasome pathway, in reducing its intracellular level. Moreover, the RNA chaperone activity of Vif was found to potentially influence temporal regulation of HIV-1 genomic RNA dimerization and reverse transcription (33). These results suggest that RNA binding plays a crucial role in Vif functions. In order to evaluate the incidence of Vif multimerization on its RNA binding properties, we characterized binding properties of Vif AALA to RNA fragments corresponding to various regions of HIV-1 genomic RNA (Table 1) and to previously identified high affinity binding sites (Table 2) (35). Globally, binding parameters analysis showed that alteration of the Vif PPLP domain reduces the overall affinity and specificity for RNAs (Tables 1 and 2). Similar results were obtained when analyzing Vif AALA binding to DNA counterparts of the primary TAR and B2 binding sites (Table 2). These results are in agreement with a recent study showing that Vif AALA binds to A3G mRNA fragments with lower affinity and specificity (26). This loss of specificity and affinity for nucleic acid binding might affect functions of Vif that are based on RNA interactions, such as particle assembly and reverse transcription (55,58,76). In this regard, it was observed that mutations reducing Vif affinity for RNA, diminished viral replication in non-permissive cells (37).

Vif binding to the upper TAR stem-loop induces a significant folding of the protein (Table 3). Interestingly, increasing the β-sheet fraction could expose hydrophobic surfaces, and thus promote protein–protein interactions. DLS experiments on wild-type Vif associated to TAR showed HMM complexes likely induced by protein oligomerization. Remarkably, Vif association with oligonucleotide B2, which has a similar affinity for Vif (35), did not lead to a significant increase of secondary structure content (Table 3). Accordingly, the size of the Vif/B2 complexes showed a mean radius 2-fold lower than the one measured for Vif/TAR under the same conditions (Figure 5). Thus, it is possible that the nucleic acid length influences Vif oligomerization (77). These results also would suggest the existence of a class of nucleic acid partners, which increases protein structure content upon binding and induces formation of HMM ribonucleoprotein complexes. Indeed, binding affinity should not be a determinant for this mode of protein/RNA interaction. Besides, different Vif/nucleic acids binding modes could correspond to different functions played by the protein during HIV-1 infection. We have previously proposed that Vif binding to viral RNA or DNA fragments could protect the genome from A3G/3F editing by a direct competition with these antiviral factors (35). Thus, despite the limited amount of Vif into viral particles, this tendency to oligomerization and to form ribonucleoprotein complexes would allow Vif to cover and protect viral nucleic acids. Moreover, we recently observed that mutations of the domain governing Vif multimerization reduced the overall affinity of the protein for A3G mRNA, but interestingly, without affecting its translation (26). Considering these new results, it would be conceivable that wild-type Vif would make use of this binding mode to inhibit ribosome scanning. Further *in vivo* studies would definitively shed light on molecular mechanisms involving the ability of Vif to bind nucleic acids and to form HMM ribonucleoprotein complexes. Unfortunately, we were not able to purify Vif AALA protein in sufficient amounts and under the conditions required for the CD analysis of protein/nucleic acid complexes. Nevertheless DLS analysis on Vif AALA binding to TAR and B2 sequences showed a similar size of ribonucleoprotein complexes in both cases. However, compared with wild-type protein, the average size of the protein/RNA complexes was almost 5-fold lower (Figure 5), thus confirming that multimerization facilitates the formation of HMM ribonucleoprotein complexes.

Beyond the genomic RNA context, Vif could make use of this property to oligomerize and form ribonucleoprotein complexes to target A3G. Indeed, A3G was

found to accumulate into punctate cytoplasmic structures described as P bodies or stress bodies (78–80), and analysis of cell lysates revealed the assembly of this antiviral factor into HMM complexes (81). Interestingly, mass spectrometry of immuno-purified HMM complexes identified a multi-subunit ribonucleoprotein complex (78,79,82) containing various RNAs such as A3G mRNA, and HIV-1 Gag mRNA in infected cells (79). Interestingly, Vif induces conversion of A3G low molecular mass complexes to presumably packaging-incompetent HMM complexes in cells (81,83,84). Beside Vif activities in A3G degradation (11,17,18,20,21,85) and inhibition of A3G translation (24–26), this sequestration mechanism would represent another mechanism to limit the antiviral effect of A3G. Taken together, our results indicate that Vif multimerization could be important for functions involving RNAs, such as viral particle assembly and reverse transcription or A3G binding and degradation (49,86). Thus, dissecting the molecular mechanisms regulating Vif–RNA interactions, including protein oligomerization, could provide novel targets for rational drugs design against HIV-1. Finally, the analysis of wild-type and mutant Vif proteins performed in this study provide information about the multimerization stage, the presence of unfolded regions, and the binding to ligands that are crucial for any attempt to solve a 3D protein structure by NMR or X-ray crystallography.

ACKNOWLEDGEMENT

We thank Bernard Lorber (Architecture et Réactivité de l'ARN, Université de Strasbourg, CNRS) for fruitful discussion on DLS experiments.

FUNDING

French 'Agence Nationale de Recherches contre le SIDA' (ANRS to J.-C.P. and R.M.); French Ministry of Higher Education and Research and of SIDACTION, fellowships (to G.M.). Funding for open access charge: French 'Agence Nationale de Recherches contre le SIDA' (ANRS).

Conflict of interest statement. None declared.

REFERENCES

1. Malim,M.H. and Emerman,M. (2008) HIV-1 accessory proteins–ensuring viral survival in a hostile environment. *Cell Host Microbe*., **3**, 388–398.
2. Sodroski,J., Goh,W.C., Rosen,C., Tartar,A., Portetelle,D., Burny,A. and Haseltine,W. (1986) Replicative and cytopathic potential of HTLV-III/LAV with sor gene deletions. *Science*, **231**, 1549–1553.
3. Gabuzda,D.H., Lawrence,K., Langhoff,E., Terwilliger,E., Dorfman,T., Haseltine,W.A. and Sodroski,J. (1992) Role of vif in replication of human immunodeficiency virus type 1 in CD4+ T lymphocytes. *J. Virol*., **66**, 6489–6495.
4. Borman,A.M., Quillent,C., Charneau,P., Dauguet,C. and Clavel,F. (1995) Human immunodeficiency virus type 1 Vif- mutant particles from restrictive cells: role of Vif in correct particle assembly and infectivity. *J. Virol*., **69**, 2058–2067.
5. Courcoul,M., Patience,C., Rey,F., Blanc,D., Harmache,A., Sire,J., Vigne,R. and Spire,B. (1995) Peripheral blood mononuclear cells produce normal amounts of defective Vif- human immunodeficiency virus type 1 particles which are restricted for the preretrotranscription steps. *J. Virol*., **69**, 2068–2074.
6. Henriet,S., Mercenne,G., Bernacchi,S., Paillart,J.C. and Marquet,R. (2009) Tumultuous relationship between the human immunodeficiency virus type 1 viral infectivity factor (Vif) and the human APOBEC-3G and APOBEC-3F restriction factors. *Microbiol. Mol. Biol. Rev*., **73**, 211–232.
7. Wissing,S., Galloway,N.L. and Greene,W.C. (2010) HIV-1 Vif versus the APOBEC3 cytidine deaminases: an intracellular duel between pathogen and host restriction factors. *Mol. Aspects Med*, in press.
8. Sheehy,A.M., Gaddis,N.C. and Malim,M.H. (2003) The antiretroviral enzyme APOBEC3G is degraded by the proteasome in response to HIV-1 Vif. *Nat. Med*., **9**, 1404–1407.
9. Wiegand,H.L., Doehle,B.P., Bogerd,H.P. and Cullen,B.R. (2004) A second human antiretroviral factor, APOBEC3F, is suppressed by the HIV-1 and HIV-2 Vif proteins. *EMBO J*., **23**, 2451–2458.
10. Mariani,R., Chen,D., Schrofelbauer,B., Navarro,F., Konig,R., Bollman,B., Munk,C., Nymark-McMahon,H. and Landau,N.R. (2003) Species-specific exclusion of APOBEC3G from HIV-1 virions by Vif. *Cell*, **114**, 21–31.
11. Yu,X., Yu,Y., Liu,B., Luo,K., Kong,W., Mao,P. and Yu,X.F. (2003) Induction of APOBEC3G ubiquitination and degradation by an HIV-1 Vif–Cul5–SCF complex. *Science*, **302**, 1056–1060.
12. Holmes,R.K., Malim,M.H. and Bishop,K.N. (2007) APOBEC-mediated viral restriction: not simply editing? *Trends. Biochem. Sci*., **32**, 118–128.
13. Hultquist,J.F. and Harris,R.S. (2009) Leveraging APOBEC3 proteins to alter the HIV mutation rate and combat AIDS. *Future Virol*., **4**, 605.
14. Yang,B., Chen,K., Zhang,C., Huang,S. and Zhang,H. (2007) Virion-associated uracil DNA glycosylase-2 and apurinic/apyrimidinic endonuclease are involved in the degradation of APOBEC3G-edited nascent HIV-1 DNA. *J. Biol. Chem*., **282**, 11667–11675.
15. Luo,K., Wang,T., Liu,B., Tian,C., Xiao,Z., Kappes,J. and Yu,X.F. (2007) Cytidine deaminases APOBEC3G and APOBEC3F interact with human immunodeficiency virus type 1 integrase and inhibit proviral DNA formation. *J. Virol*., **81**, 7238–7248.
16. Chiu,Y.L. and Greene,W.C. (2008) The APOBEC3 cytidine deaminases: an innate defensive network opposing exogenous retroviruses and endogenous retroelements. *Annu. Rev. Immunol*., **26**, 317–353.
17. Marin,M., Rose,K.M., Kozak,S.L. and Kabat,D. (2003) HIV-1 Vif protein binds the editing enzyme APOBEC3G and induces its degradation. *Nat. Med*., **9**, 1398–1403.
18. Mehle,A., Goncalves,J., Santa-Marta,M., McPike,M. and Gabuzda,D. (2004) Phosphorylation of a novel SOCS-box regulates assembly of the HIV-1 Vif–Cul5 complex that promotes APOBEC3G degradation. *Genes Dev*., **18**, 2861–2866.
19. Conticello,S.G., Langlois,M.A., Yang,Z. and Neuberger,M.S. (2007) DNA deamination in immunity: AID in the context of its APOBEC relatives. *Adv. Immunol*., **94**, 37–73.
20. Liu,B., Sarkis,P.T., Luo,K., Yu,Y. and Yu,X.F. (2005) Regulation of Apobec3F and human immunodeficiency virus type 1 Vif by Vif-Cul5-ElonB/C E3 ubiquitin ligase. *J. Virol*., **79**, 9579–9587.
21. Iwatani,Y., Chan,D.S., Liu,L., Yoshii,H., Shibata,J., Yamamoto,N., Levin,J.G., Gronenborn,A.M. and Sugiura,W. (2009) HIV-1 Vif-mediated ubiquitination/degradation of APOBEC3G involves four critical lysine residues in its C-terminal domain. *Proc. Natl. Acad. Sci. USA*, **106**, 19539–19544.
22. Opi,S., Kao,S., Goila-Gaur,R., Khan,M.A., Miyagi,E., Takeuchi,H. and Strebel,K. (2007) Human immunodeficiency virus type 1 Vif inhibits packaging and antiviral activity of a degradation-resistant APOBEC3G variant. *J. Virol*., **81**, 8236–8246.
23. Goila-Gaur,R., Khan,M.A., Miyagi,E. and Strebel,K. (2009) Differential sensitivity of "old" versus "new" APOBEC3G to

human immunodeficiency virus type 1 vif. *J. Virol.*, **83**, 1156–1160.
24. Stopak,K., de Noronha,C., Yonemoto,W. and Greene,W.C. (2003) HIV-1 Vif blocks the antiviral activity of APOBEC3G by impairing both its translation and intracellular stability. *Mol. Cell*, **12**, 591–601.
25. Kao,S., Khan,M.A., Miyagi,E., Plishka,R., Buckler-White,A. and Strebel,K. (2003) The human immunodeficiency virus type 1 Vif protein reduces intracellular expression and inhibits packaging of APOBEC3G (CEM15), a cellular inhibitor of virus infectivity. *J. Virol.*, **77**, 11398–11407.
26. Mercenne,G., Bernacchi,S., Richer,D., Bec,G., Henriet,S., Paillart,J.C. and Marquet,R. (2010) HIV-1 Vif binds to APOBEC3G mRNA and inhibits its translation. *Nucleic Acids Res.*, **38**, 633–646.
27. Tian,C., Yu,X., Zhang,W., Wang,T., Xu,R. and Yu,X.F. (2006) Differential requirement for conserved tryptophans in human immunodeficiency virus type 1 Vif for the selective suppression of APOBEC3G and APOBEC3F. *J. Virol.*, **80**, 3112–3115.
28. Simon,V., Zennou,V., Murray,D., Huang,Y., Ho,D.D. and Bieniasz,P.D. (2005) Natural variation in Vif: differential impact on APOBEC3G/3F and a potential role in HIV-1 diversification. *PLoS Pathog*, **1**, e6.
29. Dang,Y., Davis,R.W., York,I.A. and Zheng,Y.H. (2010) Identification of 81LGxGxxIxW89 and 171EDRW174 domains from human immunodeficiency virus type 1 Vif that regulate APOBEC3G and APOBEC3F neutralizing activity. *J. Virol.*, **84**, 5741–5750.
30. Chen,G., He,Z., Wang,T., Xu,R. and Yu,X.F. (2009) A patch of positively charged amino acids surrounding the human immunodeficiency virus type 1 Vif SLVx4Yx9Y motif influences its interaction with APOBEC3G. *J. Virol.*, **83**, 8674–8682.
31. Dang,Y., Wang,X., Zhou,T., York,I.A. and Zheng,Y.H. (2009) Identification of a novel WxSLVK motif in the N terminus of human immunodeficiency virus and simian immunodeficiency virus Vif that is critical for APOBEC3G and APOBEC3F neutralization. *J. Virol.*, **83**, 8544–8552.
32. Lee,T.H., Coligan,J.E., Allan,J.S., McLane,M.F., Groopman,J.E. and Essex,M. (1986) A new HTLV-III/LAV protein encoded by a gene found in cytopathic retroviruses. *Science*, **231**, 1546–1549.
33. Henriet,S., Sinck,L., Bec,G., Gorelick,R.J., Marquet,R. and Paillart,J.C. (2007) Vif is a RNA chaperone that could temporally regulate RNA dimerization and the early steps of HIV-1 reverse transcription. *Nucleic Acids Res.*, **35**, 5141–5153.
34. Henriet,S., Richer,D., Bernacchi,S., Decroly,E., Vigne,R., Ehresmann,B., Ehresmann,C., Paillart,J.C. and Marquet,R. (2005) Cooperative and specific binding of Vif to the 5′ region of HIV-1 genomic RNA. *J. Mol. Biol.*, **354**, 55–72.
35. Bernacchi,S., Henriet,S., Dumas,P., Paillart,J.C. and Marquet,R. (2007) RNA and DNA binding properties of HIV-1 Vif protein: a fluorescence study. *J. Biol. Chem.*, **282**, 26361–26368.
36. Dettenhofer,M., Cen,S., Carlson,B.A., Kleiman,L. and Yu,X.F. (2000) Association of human immunodeficiency virus type 1 Vif with RNA and its role in reverse transcription. *J. Virol.*, **74**, 8938–8945.
37. Zhang,H., Pomerantz,R.J., Dornadula,G. and Sun,Y. (2000) Human immunodeficiency virus type 1 Vif protein is an integral component of an mRNP complex of viral RNA and could be involved in the viral RNA folding and packaging process. *J. Virol.*, **74**, 8252–8261.
38. Oberste,M.S. and Gonda,M.A. (1992) Conservation of amino-acid sequence motifs in lentivirus Vif proteins. *Virus Genes*, **6**, 95–102.
39. Yu,Y., Xiao,Z., Ehrlich,E.S., Yu,X. and Yu,X.F. (2004) Selective assembly of HIV-1 Vif–Cul5–ElonginB–ElonginC E3 ubiquitin ligase complex through a novel SOCS box and upstream cysteines. *Genes Dev.*, **18**, 2867–2872.
40. Schmitt,K., Hill,M.S., Ruiz,A., Culley,N., Pinson,D.M., Wong,S.W. and Stephens,E.B. (2009) Mutations in the highly conserved SLQYLA motif of Vif in a simian-human immunodeficiency virus result in a less pathogenic virus and are associated with G-to-A mutations in the viral genome. *Virology*, **383**, 362–372.
41. Xiao,Z., Ehrlich,E., Yu,Y., Luo,K., Wang,T., Tian,C. and Yu,X.F. (2006) Assembly of HIV-1 Vif–Cul5 E3 ubiquitin ligase through a novel zinc-binding domain-stabilized hydrophobic interface in Vif. *Virology*, **349**, 290–299.
42. Mehle,A., Thomas,E.R., Rajendran,K.S. and Gabuzda,D. (2006) A zinc-binding region in Vif binds Cul5 and determines cullin selection. *J. Biol. Chem.*, **281**, 17259–17265.
43. Barraud,P., Paillart,J.C., Marquet,R. and Tisne,C. (2008) Advances in the structural understanding of Vif proteins. *Curr. HIV Res.*, **6**, 91–99.
44. Yang,S., Sun,Y. and Zhang,H. (2001) The multimerization of human immunodeficiency virus type I Vif protein: a requirement for Vif function in the viral life cycle. *J. Biol. Chem.*, **276**, 4889–4893.
45. Yang,B., Gao,L., Li,L., Lu,Z., Fan,X., Patel,C.A., Pomerantz,R.J., DuBois,G.C. and Zhang,H. (2003) Potent suppression of viral infectivity by the peptides that inhibit multimerization of human immunodeficiency virus type 1 (HIV-1) Vif proteins. *J. Biol. Chem.*, **278**, 6596–6602.
46. Auclair,J.R., Green,K.M., Shandilya,S., Evans,J.E., Somasundaran,M. and Schiffer,C.A. (2007) Mass spectrometry analysis of HIV-1 Vif reveals an increase in ordered structure upon oligomerization in regions necessary for viral infectivity. *Proteins*, **69**, 270–284.
47. Simon,J.H., Fouchier,R.A., Southerling,T.E., Guerra,C.B., Grant,C.K. and Malim,M.H. (1997) The Vif and Gag proteins of human immunodeficiency virus type 1 colocalize in infected human T cells. *J. Virol.*, **71**, 5259–5267.
48. Miller,J.H., Presnyak,V. and Smith,H.C. (2007) The dimerization domain of HIV-1 viral infectivity factor Vif is required to block virion incorporation of APOBEC3G. *Retrovirology*, **4**, 81.
49. Donahue,J.P., Vetter,M.L., Mukhtar,N.A. and D'Aquila,R.T. (2008) The HIV-1 Vif PPLP motif is necessary for human APOBEC3G binding and degradation. *Virology*, **377**, 49–53.
50. Kataropoulou,A., Bovolenta,C., Belfiore,A., Trabatti,S., Garbelli,A., Porcellini,S., Lupo,R. and Maga,G. (2009) Mutational analysis of the HIV-1 auxiliary protein Vif identifies independent domains important for the physical and functional interaction with HIV-1 reverse transcriptase. *Nucleic Acids Res.*, **37**, 3660–3669.
51. Bergeron,J.R., Huthoff,H., Veselkov,D.A., Beavil,R.L., Simpson,P.J., Matthews,S.J., Malim,M.H. and Sanderson,M.R. (2010) The SOCS-box of HIV-1 Vif interacts with ElonginBC by induced-folding to recruit its Cul5-containing ubiquitin ligase complex. *PLoS Pathog*, **6**, e1000925.
52. Wolfe,L.S., Stanley,B.J., Liu,C., Eliason,W.K. and Xiong,Y. (2010) Dissection of the HIV Vif interaction with human E3 ubiquitin ligase. *J. Virol.*, **84**, 7135–7139.
53. Goncalves,J., Shi,B., Yang,X. and Gabuzda,D. (1995) Biological activity of human immunodeficiency virus type 1 Vif requires membrane targeting by C-terminal basic domains. *J. Virol.*, **69**, 7196–7204.
54. Bouyac,M., Courcoul,M., Bertoia,G., Baudat,Y., Gabuzda,D., Blanc,D., Chazal,N., Boulanger,P., Sire,J., Vigne,R. *et al.* (1997) Human immunodeficiency virus type 1 Vif protein binds to the Pr55Gag precursor. *J. Virol.*, **71**, 9358–9365.
55. Khan,M.A., Aberham,C., Kao,S., Akari,H., Gorelick,R., Bour,S. and Strebel,K. (2001) Human immunodeficiency virus type 1 Vif protein is packaged into the nucleoprotein complex through an interaction with viral genomic RNA. *J. Virol.*, **75**, 7252–7265.
56. Bardy,M., Gay,B., Pebernard,S., Chazal,N., Courcoul,M., Vigne,R., Decroly,E. and Boulanger,P. (2001) Interaction of human immunodeficiency virus type 1 Vif with Gag and Gag–Pol precursors: co-encapsidation and interference with viral protease-mediated Gag processing. *J. Gen. Virol.*, **82**, 2719–2733.
57. Simon,J.H. and Malim,M.H. (1996) The human immunodeficiency virus type 1 Vif protein modulates the postpenetration stability of viral nucleoprotein complexes. *J. Virol.*, **70**, 5297–5305.
58. Dettenhofer,M. and Yu,X.F. (2001) Characterization of the biosynthesis of human immunodeficiency virus type 1 Env from infected T-cells and the effects of glucose trimming of Env on virion infectivity. *J. Biol. Chem.*, **276**, 5985–5991.
59. Simon,J.H., Carpenter,E.A., Fouchier,R.A. and Malim,M.H. (1999) Vif and the p55(Gag) polyprotein of human

immunodeficiency virus type 1 are present in colocalizing membrane-free cytoplasmic complexes. *J. Virol.*, **73**, 2667–2674.
60. Stanley,B.J., Ehrlich,E.S., Short,L., Yu,Y., Xiao,Z., Yu,X.F. and Xiong,Y. (2008) Structural insight into the human immunodeficiency virus Vif SOCS box and its role in human E3 ubiquitin ligase assembly. *J. Virol.*, **82**, 8656–8663.
61. Balaji,S., Kalpana,R. and Shapshak,P. (2006) Paradigm development: comparative and predictive 3D modeling of HIV-1 virion infectivity factor (Vif). *Bioinformation*, **1**, 290–309.
62. Lv,W., Liu,Z., Jin,H., Yu,X. and Zhang,L. (2007) Three-dimensional structure of HIV-1 VIF constructed by comparative modeling and the function characterization analyzed by molecular dynamics simulation. *Org. Biomol. Chem.*, **5**, 617–626.
63. Paul,I., Cui,J. and Maynard,E.L. (2006) Zinc binding to the HCCH motif of HIV-1 virion infectivity factor induces a conformational change that mediates protein–protein interactions. *Proc. Natl Acad. Sci. USA*, **103**, 18475–18480.
64. Giri,K. and Maynard,E.L. (2009) Conformational analysis of a peptide approximating the HCCH motif in HIV-1 Vif. *Biopolymers*, **92**, 417–425.
65. Reingewertz,T.H., Benyamini,H., Lebendiker,M., Shalev,D.E. and Friedler,A. (2009) The C-terminal domain of the HIV-1 Vif protein is natively unfolded in its unbound state. *Protein Eng. Des. Sel.*, **22**, 281–287.
66. Scatchard,G. (1949) The attraction of proteins for small ions and molecules. *Ann. N Y Acad. Sci.*, **51**, 660–672.
67. McGhee,J.D. and von Hippel,P.H. (1974) Theoretical aspects of DNA–protein interactions: co-operative and non-co-operative binding of large ligands to a one-dimensional homogeneous lattice. *J. Mol. Biol.*, **86**, 469–489.
68. Tsodikov,O.V., Holbrook,J.A., Shkel,I.A. and Record,M.T. Jr (2001) Analytic binding isotherms describing competitive interactions of a protein ligand with specific and nonspecific sites on the same DNA oligomer. *Biophys. J.*, **81**, 1960–1969.
69. Chen,Y. and Barkley,M.D. (1998) Toward understanding tryptophan fluorescence in proteins. *Biochemistry*, **37**, 9976–9982.
70. Lakowicz,J.R. (1999) In Lakowicz,J.R. (ed.), *Principles of Fluorescence Spectroscopy*, 2nd edn. Plenum Press, NY.
71. Baudin,F., Marquet,R., Isel,C., Darlix,J.L., Ehresmann,B. and Ehresmann,C. (1993) Functional sites in the 5′ region of human immunodeficiency virus type 1 RNA form defined structural domains. *J. Mol. Biol.*, **229**, 382–397.
72. Reingewertz,T.H., Shalev,D.E. and Friedler,A. (2010) Structural disorder in the HIV-1 Vif protein and interaction-dependent gain of structure. *Protein Pept. Lett.*, **17**, 988–998.
73. Fink,A.L. (2005) Natively unfolded proteins. *Curr. Opin. Struct. Biol.*, **15**, 35–41.
74. Wright,P.E. and Dyson,H.J. (1999) Intrinsically unstructured proteins: re-assessing the protein structure-function paradigm. *J. Mol. Biol.*, **293**, 321–331.
75. Dyson,H.J. and Wright,P.E. (2004) Unfolded proteins and protein folding studied by NMR. *Chem. Rev.*, **104**, 3607–3622.
76. Ohagen,A. and Gabuzda,D. (2000) Role of Vif in stability of the human immunodeficiency virus type 1 core. *J. Virol.*, **74**, 11055–11066.
77. Stoylov,S.P., Vuilleumier,C., Stoylova,E., De Rocquigny,H., Roques,B.P., Gerard,D. and Mely,Y. (1997) Ordered aggregation of ribonucleic acids by the human immunodeficiency virus type 1 nucleocapsid protein. *Biopolymers*, **41**, 301–312.
78. Gallois-Montbrun,S., Kramer,B., Swanson,C.M., Byers,H., Lynham,S., Ward,M. and Malim,M.H. (2007) Antiviral protein APOBEC3G localizes to ribonucleoprotein complexes found in P bodies and stress granules. *J. Virol.*, **81**, 2165–2178.
79. Kozak,S.L., Marin,M., Rose,K.M., Bystrom,C. and Kabat,D. (2006) The anti-HIV-1 editing enzyme APOBEC3G binds HIV-1 RNA and messenger RNAs that shuttle between polysomes and stress granules. *J. Biol. Chem.*, **281**, 29105–29119.
80. Wichroski,M.J., Robb,G.B. and Rana,T.M. (2006) Human retroviral host restriction factors APOBEC3G and APOBEC3F localize to mRNA processing bodies. *PLoS Pathog*, **2**, e41.
81. Chiu,Y.L., Soros,V.B., Kreisberg,J.F., Stopak,K., Yonemoto,W. and Greene,W.C. (2005) Cellular APOBEC3G restricts HIV-1 infection in resting CD4+ T cells. *Nature*, **435**, 108–114.
82. Chiu,Y.L. and Greene,W.C. (2006) Multifaceted antiviral actions of APOBEC3 cytidine deaminases. *Trends Immunol.*, **27**, 291–297.
83. Goila-Gaur,R., Khan,M.A., Miyagi,E., Kao,S., Opi,S., Takeuchi,H. and Strebel,K. (2008) HIV-1 Vif promotes the formation of high molecular mass APOBEC3G complexes. *Virology*, **372**, 136–146.
84. Soros,V.B. and Greene,W.C. (2007) APOBEC3G and HIV-1: strike and counterstrike. *Curr. HIV/AIDS Rep.*, **4**, 3–9.
85. Conticello,S.G., Harris,R.S. and Neuberger,M.S. (2003) The Vif protein of HIV triggers degradation of the human antiretroviral DNA deaminase APOBEC3G. *Curr. Biol.*, **13**, 2009–2013.
86. Walker,R.C. Jr, Khan,M.A., Kao,S., Goila-Gaur,R., Miyagi,E. and Strebel,K. (2010) Identification of dominant negative human immunodeficiency virus type 1 Vif mutants that interfere with the functional inactivation of APOBEC3G by virus-encoded Vif. *J. Virol.*, **84**, 5201–5211.